

# The H I Environment of Nearby Lyman-alpha Absorbers

J. H. van Gorkom

Department of Astronomy, Columbia University, NY 10027

C. L. Carilli

National Radio Astronomy Observatory, P.O. Box O, Socorro, NM 87801

John T. Stocke, Eric S. Perlman<sup>1</sup>, and J. Michael Shull <sup>2</sup>

Center for Astrophysics and Space Astronomy, Department of Astrophysical, Planetary, and  
Atmospheric Sciences, University of Colorado, Boulder, CO 80309

Received \_\_\_\_\_; accepted \_\_\_\_\_

---

<sup>1</sup> now at Laboratory for High Energy Astrophysics, NASA-Goddard Space Flight Center,  
Mail Code 660.2, Greenbelt, MD 20771

<sup>2</sup>also at JILA, University of Colorado and National Institute of Standards and Technology

## ABSTRACT

We present the results of a VLA and WSRT search for H I emission from the vicinity of seven nearby clouds, which were observed in Ly $\alpha$  absorption with HST toward Mrk 335, Mrk 501 and PKS 2155-304. Around the absorbers, we searched a volume of  $40' \times 40' \times 1000 \text{ km s}^{-1}$ ; for one of the absorbers we probed a velocity range of only  $600 \text{ km s}^{-1}$ . The H I mass sensitivity ( $5 \sigma$ ) very close to the lines of sight varies from  $5 \times 10^6 \text{ M}_\odot$  at best to  $5 \times 10^8 \text{ M}_\odot$  at worst.

We detected H I emission in the vicinity of four out of seven absorbers. The closest galaxy we find to the absorbers is a small dwarf galaxy at a projected distance of  $68h^{-1} \text{ kpc}$  from the sight line toward Mrk 335. This optically uncataloged galaxy has the same velocity ( $V = 1970 \text{ km s}^{-1}$ ) as one of the absorbers, is fainter than the SMC, and has an H I mass of only  $4 \times 10^7 \text{ M}_\odot$ . We found a somewhat more luminous galaxy at exactly the velocity ( $V = 5100 \text{ km s}^{-1}$ ) of one of the absorbers toward PKS 2155-304 at a projected distance of  $230h^{-1} \text{ kpc}$  from the sight line. Two other, stronger absorbers toward PKS 2155-304 at  $V \approx 17,000 \text{ km s}^{-1}$  appear to be associated with a loose group of three bright spiral galaxies, at projected distances of 300 to  $600h^{-1} \text{ kpc}$ . These results support the conclusions emerging from optical searches that most nearby Ly $\alpha$  forest clouds trace the large-scale structures outlined by the optically luminous galaxies, although this is still based on small-number statistics. We do not find any evidence from the H I distribution or kinematics that there is a physical association between an absorber and its closest galaxy. While the absorbing clouds are at the systemic velocity of the galaxies, the H I extent of the galaxies is fairly typical, and at least an order of magnitude smaller than the projected distance to the sight line at which the absorbers are seen. On the other hand, we also do not find evidence against such a connection.

In total, we detected H I emission from five galaxies, of which two were previously uncataloged and one did not have a known redshift. No H I emission was detected from the vicinity of the two absorbers, which are located in a void and a region of very low galaxy density; but the limits are somewhat less stringent than for the other sight lines. These results are similar to what has been found in optically unbiased H I surveys. Thus, the presence of Ly $\alpha$  absorbers does not significantly alter the H I detection rate in their environment.

## 1. Introduction

The plethora of low column density, intervening Ly $\alpha$  absorption lines in the spectra of high redshift QSO's (the “Ly $\alpha$  forest”) was first recognized by Lynds (1971) and has been described in detail by Sargent et al. (1980) and in many recent reviews and articles (Bajtlik 1993; Weymann 1993; Bechtold 1993; Rauch et al. 1992; Rauch et al. 1993; Lu, Wolfe, & Turnshek 1991; Smette et al. 1992). A considerable amount has been learned about the nature of these systems at redshifts  $z \geq 1.6$ , the redshift above which Ly $\alpha$  is observable from the ground. These redshifts are generally too large to directly detect the absorbing objects in emission. However, more recently, a modest number of Ly $\alpha$  absorbers at low redshift have been detected in the UV (Morris et al. 1991; Bahcall et al. 1991). The proximity of these systems make them ideal targets for searches for H I and optical emission from the vicinity of these clouds. One can also seek possible identifications of parent objects with which the clouds might be associated.

The first low-redshift Ly $\alpha$  forest absorption lines were discovered in the IUE spectrum of PKS 2155-304 by Maraschi et al. (1988). Since then, the HST has revealed many low column density absorbers in the nearby universe (Bahcall et al. 1991; Bahcall et al. 1993; Morris et al. 1991; Bruhweiler et al. 1993; Stocke et al. 1995; Shull et al. 1996). Statistical studies have been made to determine the relative correlation between these Ly $\alpha$  absorbing clouds and optical galaxies (Morris et al. 1991; Salzer 1992; Stocke et al. 1995; Lanzetta et al. 1995; Mo & Morris 1994; Morris et al. 1993; Morris & van den Bergh 1994). The current consensus is that the systems do correlate weakly with bright galaxies, but less so than these galaxies with other galaxies (Stocke et al. 1995). Lanzetta et al. (1995) find good evidence that some of the stronger Ly $\alpha$  absorbers are physically close to galaxies, but there are also examples of clouds with no optical galaxy to within a few Mpc (Stocke et al. 1995; Shull et al. 1996). Morris et al. (1991) find, in one instance, an anti-correlation between a

region of very high galaxy density and Ly $\alpha$  forest absorbing clouds. Stocke et al. (1995) find more generally that: “the higher equivalent width absorbers are distributed more like galaxies than the lower equivalent width absorbers, which are distributed in a manner statistically indistinguishable from clouds randomly placed with respect to galaxies.”

In this paper, we present a search for H I emission from the vicinity of seven nearby Ly $\alpha$  absorbers. H I imaging surveys routinely find gas-rich, optically uncataloged galaxies, and as such our search is complementary to the optical surveys mentioned above. In addition to searching for a possible parent population of the Ly $\alpha$  absorbers, the H I morphology of galaxies close to the line of sight might betray hints of unusually large gaseous extents. In the first study of this kind (van Gorkom et al. 1993) a deep search for H I emission was made around two Ly $\alpha$  clouds on the 3C 273 line of sight, which are located in the outskirts of the Virgo Cluster. No obvious associations between these two Ly $\alpha$  clouds and H I emitting galaxies were found. The seven systems studied here are located in a wide range of cosmic environments. The absorbers seen along the sight line toward Mrk 501 are located in a void and a very low density region, respectively, while the other five absorbers are located in regions of moderately high galaxy density, along the sight lines toward PKS 2155-304 and Mrk 335. The results of the H I search near the sight line toward Mrk 501 have already been presented by Stocke et al. (1995). Here, those observations will be presented in somewhat more detail. We describe the systems and observations in § 2 and § 3. We present the results in § 4, and in § 5 we briefly discuss their implications.

Throughout this paper we adopt heliocentric velocities, using the optical definition,  $V_{opt} = cz$ , where  $c$  is the speed of light and the redshift is defined as  $z = \frac{\lambda - \lambda_0}{\lambda_0}$ , where  $\lambda$  and  $\lambda_0$  are the observed and rest wavelengths, respectively.

## 2. The Systems

The seven absorption-line systems have been discovered by different authors and their properties can be found in the literature. In Table 1 we summarize the sources against which they have been found, the heliocentric velocities of the lines, and the measured equivalent widths. In this Table we also give the projected distance to our H I detection closest to the line of sight and the difference between the velocity of the absorption line and the systemic velocity of the galaxy as derived from the H I.

Two of the systems are seen in absorption against the BL Lac object Mrk 501, which is located in the “Great Wall” of galaxies at heliocentric velocity  $10,300 \text{ km s}^{-1}$ . The two absorbing systems are at  $7530 \text{ km s}^{-1}$  and  $4660 \text{ km s}^{-1}$  (Stocke et al. 1995). The  $7530 \text{ km s}^{-1}$  system is located in the void between us and the great wall, it has no cataloged optical galaxies within  $4.5h^{-1} \text{ Mpc}$ , where  $h$  is the Hubble constant in units of  $100 \text{ km s}^{-1} \text{ Mpc}^{-1}$ . The  $4670 \text{ km s}^{-1}$  system has a sparse chain of galaxies located to the southwest, the closest of which is  $25'$  ( $340h^{-1} \text{ kpc}$ ) off the line of sight to Mrk 501.

The detections of five, and possibly six, local Ly $\alpha$  forest lines have been reported for the sight line toward the BL Lac object PKS 2155-304 (Bruhweiler et al. 1993; Maraschi et al. 1988; Allen et al. 1993). We did an H I search around the three stronger lines, at  $5100 \text{ km s}^{-1}$ ,  $16,488 \text{ km s}^{-1}$  and  $17,088 \text{ km s}^{-1}$  respectively. The last two velocities are uncertain by about  $140 \text{ km s}^{-1}$ . The lower velocity system is on the edge of the Perseus – Pisces supercluster; its nearest cataloged galaxy is ESO 466-G032,  $15'$  ( $230h^{-1} \text{ kpc}$ ) east of the sight line toward PKS 2155-304 with a systemic velocity of  $5187 \text{ km s}^{-1}$ . The higher velocity systems have a number of cataloged galaxies at similar velocities not far from the line of sight. The closest is 2155-3033 (from the CfA redshift catalog), an Sb spiral  $6.4'$  ( $305h^{-1} \text{ kpc}$ ) to the SW of the line of sight to PKS 2155-304 and with a systemic velocity of  $17,300 \text{ km s}^{-1}$ .

The third sight line that we investigated is toward Mrk 335, which has four Ly $\alpha$

absorption lines (Stocke et al. 1995). Here, we observed the two lower velocity systems, which are close together in velocity at 1970 and 2290 km s<sup>−1</sup>. These systems are located in a supercluster region. The closest cataloged galaxy is NGC 7817, an SAbc spiral, 46.5' (311h<sup>−1</sup> kpc) to the NE of the sight line toward Mrk 335 and with a systemic velocity of 2309 km s<sup>−1</sup>.

The H I column densities for the absorbing systems are all in the range of 10<sup>13–14</sup> cm<sup>−2</sup> (assuming a Doppler parameter  $b = 30$  km s<sup>−1</sup>), except for the complex absorption lines around 17,000 km s<sup>−1</sup>. For these, a large column density,  $\sim 10^{18}$  cm<sup>−2</sup>, has been derived (Maraschi et al. 1988), placing it in the lower column density range of heavy element quasar absorption line systems. Thus far, no firm detections of metal lines have been made in this system, implying a metallicity < 0.1 solar (Bruhweiler et al. 1993).

### 3. Observations and Data Processing

One of the sight lines, the one toward Mrk 501, was observed with the Westerbork Synthesis Radio Telescope (WSRT), while the other searches were done with the Very Large Array (VLA). We describe the observations and data processing for each of the sight lines separately. Table 2 summarizes the observations.

#### 3.1. Mrk 501

The two Ly $\alpha$  absorption systems towards Mrk 501 were observed with the WSRT. Two 12 hour synthesis observations were made centered at 4885 km s<sup>−1</sup> with short spacings of 36 m and 54 m, and a single 12 hour synthesis observation, centered at 7740 km s<sup>−1</sup>. The

total velocity range covered in each case was  $1000 \text{ km s}^{-1}$  at a resolution of  $17 \text{ km s}^{-1}$ . Standard calibration of the data was performed using the NEWSTAR data reduction software package at NFRA. Further data editing, imaging, and analysis were performed using the AIPS package.

Mrk 501 is a radio continuum source, with an observed flux density at 1.4 GHz of 1.3 Jy. The source is unresolved at  $15''$  resolution, with a position of  $16^{\text{h}} 52^{\text{m}} 11.65^{\text{s}}$ ,  $39^{\circ} 50' 27.1''$  (B1950). For the high-velocity system, the pointing center corresponded to the position of the continuum source, while the observations at  $4675 \text{ km s}^{-1}$  were made pointing  $5'$  to the southwest of Mrk 501 in order to increase sensitivity at the sparse chain of galaxies to the southwest.

Subtraction of the continuum emission from the line data was performed in two ways. The first involved linear fits in frequency to the calibrated complex visibilities (Cornwell et al. 1992). The second involved linear fits in frequency to the multi-channel image cube. The results from the two methods were similar, although the residual artifacts towards the edges of the field were worse for the image-plane subtraction (as expected), and the analysis presented herein relies on the uv-data continuum subtraction method.

Images of Mrk 501 were made using “natural” weighting of the visibilities. The FWHM of the WSRT synthesized beam was  $25'' \times 15''$ . The image cubes were smoothed in velocity to  $34 \text{ km s}^{-1}$  resolution and visually inspected for 21 cm emission signal. No H I signal is seen anywhere in the cube above five times the RMS in a given channel. The image cube was then smoothed in both velocity and spatially to  $68 \text{ km s}^{-1} \text{ channel}^{-1}$  and to  $38''$  spatial resolution. Again, no emission is seen anywhere in the cubes above five times the RMS at any velocity or spatial resolution. The noise values at various resolutions are listed in Table 3.

### 3.2. PKS 2155-304

PKS 2155-304 was observed twice with the VLA. The first set of observations was done with the 1 km array with an extended (3 km) north arm (DnC configuration) to compensate for the southern declination of the source. The low-velocity system was observed for 4 hours, centered at  $5100 \text{ km s}^{-1}$ , covering  $560 \text{ km s}^{-1}$  with a velocity resolution of  $21 \text{ km s}^{-1}$ . The high velocity systems were observed for a total of 10 hours. These observations were centered at  $17,400 \text{ km s}^{-1}$  in an effort to also include a possible Ly $\alpha$  system at  $17,700 \text{ km s}^{-1}$ . However, more recent HST data, obtained with the Faint Object Spectrograph and G130H grating do not confirm the reality of that system (Allen et al. 1993). The total velocity range covered was  $620 \text{ km s}^{-1}$  with a velocity resolution of  $23 \text{ km s}^{-1}$ . All those data suffered from rather serious interference. The high velocity system was reobserved with the VLA in the 1 km (D) configuration to make up for the loss of data due to interference and to cover also the Ly $\alpha$  system at  $16,488 \text{ km s}^{-1}$ . The time on source was again 10 hours. The observations were centered at  $16,880 \text{ km s}^{-1}$  and covered  $1280 \text{ km s}^{-1}$  with a resolution of  $46 \text{ km s}^{-1}$ . Unfortunately, these observations were made during daytime and the data suffered rather badly from solar interference.

PKS 2155-304 is a radio continuum source, with a variable flux density. We measured a flux density of 0.45 Jy at 1.4 GHz. All observations were centered at the radio position of the BL Lac object,  $21^{\text{h}} 55^{\text{m}} 58.30^{\text{s}}$ ,  $-30^{\circ} 27' 54.4''$  (B1950). Standard calibration procedures were followed, giving special care to the bandpass calibration. A bandpass calibrator was observed once every 2 hours, and for each data point we used the bandpass solution closest in time. Initially, we subtracted the continuum by making a linear fit in frequency to the calibrated complex visibilities, using the inner 75% of the band. After the continuum subtraction, the data were clipped to remove solar and man-made interference. Images were made of each of the observing runs separately. After inspection of the cubes to locate the

channels with H I emission, the subtraction of the continuum was redone, making a fit to the line free channels only.

For the low velocity system, images were made using natural weighting, resulting in a FWHM of the synthesized beam of  $66'' \times 39''$ . For the high-velocity systems the data of the various observing runs were combined in the UV plane, after Hanning smoothing the data of the first run down to the resolution of the second run. Images were made using natural weighting, resulting in a synthesized beam of  $97.8'' \times 47.2''$ . Several galaxies were detected in H I, one in the low-velocity data and three in the high-velocity data. These results are described in § 4.

### 3.3. Mrk 335

We observed Mrk 335 with the VLA in the 1 km (D) array for 4 hours in total. The observations were centered at  $2135 \text{ km s}^{-1}$  in between the velocities of the two Ly $\alpha$  absorbers, covering a range of  $1000 \text{ km s}^{-1}$  with a velocity resolution of  $25 \text{ km s}^{-1}$ . The observations were centered at the optical position of the Seyfert galaxy, at  $00^{\text{h}} 03^{\text{m}} 45.2^{\text{s}}$ ,  $19^{\circ} 55' 28.6''$  (B1950). The Seyfert galaxy itself is not a radio continuum source. We subtracted background continuum sources by making a linear fit to the calibrated complex visibilities. Images were made using natural weighting, resulting in a synthesized beam of  $62.8'' \times 52.7''$ . One previously uncataloged galaxy was discovered in H I. We describe this result in the next section.

For the H I detections, we made images of the total hydrogen emission by smoothing the data spatially and in velocity, using the smoothed cube as a mask for the full resolution data. Only pixels above  $2 \sigma$  in the smoothed cube were used in the sum. Throughout this paper we use images of the digitized POSS to show overlays of neutral hydrogen emission

on optical images.

## 4. Results

### 4.1. Upper Limits

Although the more interesting result of this work is the detection of so many galaxies, the upper limits we can place on any H I in emission close to the Ly $\alpha$  absorbers are important too. In Table 3 we list the mass and column density limits for each of the systems. These are  $5\sigma$  limits at the field center. Farther from the center, they need to be corrected for the change in primary beam response. The primary beam pattern is roughly Gaussian with a FWHM of  $36'$  and  $30'$  for the WSRT and the VLA respectively. For example, the VLA limits are a factor of two worse at  $15'$  from the field center, and 10 times worse at  $25'$ . At the position of the sparse group to the SW of Mrk 501, the mass and column density limits are a factor of five worse than at the field center. Although these limits put serious constraints on the presence of small, gas-rich dwarf galaxies very close to each of the lines of sight, the small dwarf detected toward Mrk 335 at  $12'$  from the line of sight could only have been detected in the observations toward Mrk 335 and in the low-velocity system toward PKS 2155-304. Interestingly, in both these observations (and only those) a small galaxy was found very close to the velocity of the absorber, but at rather large projected distance from the line of sight. It should also be noted that in the sight line toward Mrk 501, the one observation in which no galaxies were detected at all the surface brightness sensitivity is ten times worse than that of the other observations. In fact, some of the most gas-rich, but low H I surface density galaxies such as Malin 1 could have escaped detection in those data.

## 4.2. H I Detections

### 4.2.1. *Mrk 335*

Perhaps the most exciting result of these observations is the detection of the small dwarf near the sight line toward Mrk 335. Contour images of the velocity channels are shown in Fig. 1. Although the emission is not resolved in individual channels, the peak of the emission clearly shifts in position with velocity. The maximum displacement of the peaks gives us a lower limit to the H I extent, which is  $45''$  or  $4.2h^{-1}$  kpc. A position – velocity profile along the major axis of the galaxy (at a PA of  $0^\circ$ ) is shown in Fig. 2. To put things in perspective, we show in Fig. 3 an overlay of the total H I emission onto an optical image, which includes Mrk 335 as well. Although the H I is more extended than the optical emission of this tiny dwarf galaxy, there is a huge distance ( $68h^{-1}$  kpc) between the lowest H I contour (at  $4.8 \times 10^{19}$  cm $^{-2}$ ) and the sight line toward Mrk 335. The H I properties derived from this observation are summarized in Table 4. The systemic velocity as derived from the H I differs by only 20 km s $^{-1}$  from that of the higher column density absorber at 1970 km s $^{-1}$ .

### 4.2.2. *PKS 2155-304*

At low velocities, we detect H I emission from ESO 466-G032, located  $230h^{-1}$  kpc to the east of the line of sight to PKS 2155-304. This is the closest optically cataloged galaxy to the line of sight. The H I is seen over the velocity range 5080 km s $^{-1}$  to 5130 km s $^{-1}$ . Contour images of the velocity channels at 11.7 km s $^{-1}$  resolution are shown in Fig. 4. Crosses mark the optical position of the H I emitting galaxy. The systemic velocity

as derived from the H I profile is  $5100 \text{ km s}^{-1}$ , significantly less than the reported optical value of  $5187 \text{ km s}^{-1}$ . Optically, the galaxy looks rather disturbed, with a spiral arm (or tidal feature?) extending to the southwest. The H I emission is just barely above the noise. Although it appears to be slightly extended in the direction of the extended optical feature, the synthesized beam is extended in the same direction. There is a hint of rotation along the optical major axis of the galaxy, with the receding side to the northeast (Fig. 4). The angular resolution of the current data is not sufficient to say any more about the H I morphology; the signal is only barely resolved. The H I parameters are summarized in Table 4. Again, to put things in perspective we show in Fig. 5 an H I overlay on an optical image including both the galaxy and the BL Lac object.

The high-velocity data cube covers the velocity range from  $16,240 \text{ km s}^{-1}$  to  $17,720 \text{ km s}^{-1}$ , but the quality varies across the band. At velocities in excess of  $17,500 \text{ km s}^{-1}$ , the data quality is poor. We detect H I emission from three galaxies. The galaxy closest to the line of sight, 2155-3033, is at a projected distance of  $305h^{-1} \text{ kpc}$  to the south. The H I emission from this galaxy is barely above the noise. A weak signal is seen over velocities from  $16,900 \text{ km s}^{-1}$  to  $17,300 \text{ km s}^{-1}$ , with no detectable H I in the two middle channels (Fig. 6). The systemic velocity derived from the H I is  $17,100 \text{ km s}^{-1}$ , the optical redshift gives a velocity of  $17,300 \text{ km s}^{-1}$ .

A much stronger H I emitter is found to the southeast at a projected distance of  $610h^{-1} \text{ kpc}$ . This is an IRAS source, F21569-330, with a hitherto unknown redshift. The H I emission can be seen over a velocity range from  $16,650 \text{ km s}^{-1}$  to  $16,925 \text{ km s}^{-1}$  (Fig. 7). The kinematic major axis lies along the optical major axis at a PA of  $-40^\circ$ , with the north side receding. A position velocity profile along the major axis is shown in Fig. 8.

Almost due north of PKS 2155-304 we detect an optically uncataloged galaxy at a projected distance of  $515h^{-1} \text{ kpc}$  from the line of sight. H I can be seen in emission from

17,063 km s<sup>-1</sup> to 17,248 km s<sup>-1</sup> (Fig. 9). The kinematic major axis is east – west and a position velocity profile along this axis is shown in Fig. 10. Optically the galaxy looks distorted, slightly extended to the northwest with what are possibly two dwarf companions. The H I parameters derived from these observations are listed in Table 4. Finally, to put things in perspective, we show in Fig. 11 an overlay of the H I emission of the three galaxies detected in the high velocity cube on an optical image, which shows, in addition to the galaxies, PKS 2155-304.

## 5. Discussion

Our search for H I emission from the vicinity of nearby Ly $\alpha$  absorbers has resulted in the detection of five galaxies, two of which were previously uncataloged. We shall first discuss whether this detection rate is unusual in any sense: does the presence of a Ly $\alpha$  absorber increase the chance of finding H I in emission? Following that, we shall discuss what we have learned from the detections, and whether there is any indication that the H I in emission is related to the Ly $\alpha$  absorption. Finally we will discuss whether the present observations have illuminated the nature of the nearby Ly $\alpha$  absorbers.

A variety of data is available to assess whether our detection rate of H I-rich systems is unusual in any way. Briggs (1990) summarized the results of all major unbiased H I surveys, while the currently most accurate H I luminosity function has been constructed by Rao & Briggs (1993). More specific and directly comparable to our result is the work by Weinberg et al. (1991) and Szomoru et al. (1994, 1996), who used the VLA to do unbiased H I surveys in environments of differing galaxian density. Szomoru et al. (1994) probed voids as well as supercluster environments and compared fields centered on optically known galaxies and optically blank fields.

For simplicity sake, we take as the volume searched in our survey the region within a radius of  $22'$  from the pointing center. This is the 20% point of the primary beam; beyond that, the shape of the beam is highly uncertain. Our search within that volume is complete to the  $5\sigma$  limits listed in Table 3, multiplied by five (correcting for the primary beam response). The volume searched down to a mass limit of  $2 \times 10^9 M_\odot$  of H I is  $60h^{-3} \text{ Mpc}^3$ . In this volume, we detected three galaxies with H I masses of a few times  $10^9 M_\odot$  of H I, giving a density of  $0.05 \pm 0.02 \text{ Mpc}^{-3}$ . The volume searched down to  $5 \times 10^8 M_\odot$  of H I is much smaller,  $6.8h^{-3} \text{ Mpc}^3$ . Two galaxies of even smaller masses were detected in that volume, bringing the galaxy density in the mass range of  $10^7 M_\odot$  to  $5 \times 10^8$  to  $0.3 \pm 0.2h^3 \text{ Mpc}^{-3}$ . These H I mass densities are quite consistent with the results of Briggs (1990), who found a density of  $0.07h^3 \text{ Mpc}^{-3}$  and  $0.1h^3 \text{ Mpc}^{-3}$  for H I masses of a few times  $10^9 M_\odot$  and  $10^8 M_\odot$  respectively. Only a small fraction of the volume searched,  $7h^{-3} \text{ Mpc}^3$ , is in a true void; the remaining volume is more characteristic of supercluster densities. Weinberg et al. (1991) found a cumulative space density of  $0.13h^3 \text{ Mpc}^{-3}$  for gas rich dwarfs above  $10^8 M_\odot$  of H I in the Perseus – Pisces supercluster, a result similar to ours. In conclusion, although the statistics are small, it appears that the presence of nearby Ly $\alpha$  forest absorbers has not significantly altered the detection rate of H I emitting objects in either the void or the high-density regions.

### 5.1. The Markarian 335 Sight Line

Nevertheless, the detections of two galaxies almost exactly at the velocity of their nearby Ly $\alpha$  absorbers, and the fact that these are the only detections in a 500 and 1000  $\text{km s}^{-1}$  range for PKS 2155-304 and Mrk 335 respectively, beg the question whether there is a possible association between the galaxies and the absorbers. The most tantalizing system is the uncataloged dwarf galaxy at a projected distance of  $68h^{-1} \text{ kpc}$  from the line

of sight toward Mrk 335. The absolute magnitude of this dwarf has been estimated to be  $M_R \approx -15.4$  based upon a linear extrapolation of the calibration supplied by eight, nearby HST guide stars on the digitized version of the POSS-E plate material. This approximate magnitude assumes that  $H_0 = 100 \text{ km s}^{-1} \text{ Mpc}^{-1}$  despite the location of this object within the bounds of the local supercluster. The proximity, spatially and in velocity, of the Ly $\alpha$  absorber and dwarf irregular could mean no more than that they originated in a common larger scale structure, e.g., a filament (Cen et al. 1994; Hernquist et al. 1996; Miralda-Escudé et al. 1996; Mücke et al. 1996). Alternatively, it could imply that the Ly $\alpha$  cloud is gravitationally bound to the dwarf. Perhaps, it is still falling in or has been ejected in a galactic wind. The kinematic structure does not help to choose between these various possibilities. The minimum dynamical mass in the Ly $\alpha$  cloud + dwarf galaxy system needed to make it a bound system can be derived by requiring that the total kinetic energy of the system is less or equal to the potential energy. Thus,

$$M_{dyn} = \frac{1}{2G}(\Delta V)^2 \Delta R \quad (1)$$

where  $G$  is the gravitational constant,  $\Delta V$  the line-of-sight velocity difference and  $\Delta R$  the projected distance between absorber and galaxy. The minimum dynamical mass is  $4.6 \times 10^9 M_\odot$ . A crude estimate of the mass of the dwarf galaxy can be obtained from the H I kinematics. Assuming a total H I extent of 3.8 kpc and a rotation velocity of  $55 \text{ km s}^{-1}$ , we find  $M = 6.7 \times 10^8 M_\odot$ . Thus, in order for the Ly $\alpha$  cloud to be bound to the galaxy, the dwarf needs to be embedded in a massive dark halo.

An intriguing possibility is that the Ly $\alpha$  absorption arises from within a mostly ionized gas disk of the dwarf galaxy. Maloney (1992) and Stocke et al. (1995) discussed the possibility that nearby Ly $\alpha$  lines could be produced by gas at large radii in the disks of spiral and irregular galaxies. Maloney concludes that the unexpectedly large number

of low-redshift Ly $\alpha$  absorption lines seen with HST toward 3C 273 can be produced by extended ionized gas disks in the halos of spiral and irregular galaxies. The observed frequency of absorbers requires that either  $L_*$  galaxies have huge (several hundred kpc) halos or, more plausibly, that the decrease of absorption cross section with declining luminosity is slow enough for low-luminosity galaxies to dominate the integrated cross section. Shull et al. (1996) make the case that, for absorbers of mean radius  $R = (100 \text{ kpc})R_{100}$ , only dwarf galaxies have the comoving space densities,

$$\phi_0 \approx (0.9 \text{ Mpc}^{-3})R_{100}^{-2}h \quad (2)$$

necessary to explain the frequency of low-redshift Ly $\alpha$  clouds. For reference, this density is over 20 times that of  $L_*$  galaxies, recently estimated as  $\phi(L_*) \approx 0.04h^3 \text{ Mpc}^{-3}$  (Marzke et al. 1994).

A first hint that low-luminosity galaxies may indeed dominate the cross section comes from the discovery (Barcons et al. 1995) of possibly corotating Ly $\alpha$  absorption at large (50 kpc) projected distance from two small, late-type spiral galaxies. Contrary to the cases found by Barcons et al. (1995), we have no evidence for corotation of the ionized gas with the galaxy, the Ly $\alpha$  absorption occurs too close to the minor axis of the galaxy. The small velocity difference between the absorber and the systemic velocity of the galaxy is of course not inconsistent with corotation, but at that large distance anything that is bound to the galaxy is expected to have a velocity close to the systemic velocity of the galaxy.

Although Stocke et al. (1995) discussed the problems with huge ionized halos around a single bright spiral galaxy, it might be possible that the Ly $\alpha$  absorption at  $68h^{-1}$  kpc from the dwarf arises in an ionized halo. Using the model calculations of Maloney (1992) and Dove & Shull (1994), we find that an ionized 80–100 kpc halo is not at all unlikely for a dwarf galaxy. For example, consider a spherical dark-matter halo, with central density  $\rho_0$ , core radius  $r_c$ , and asymptotic halo velocity  $v_A = (4\pi G \rho_0 r_c^2)^{1/2} \equiv (50 \text{ km s}^{-1})v_{50}$ .

The three-dimensional velocity dispersion is  $\langle v^2 \rangle = (3/2)v_A^2$ . In equilibrium, the gaseous hydrogen will settle into an atmosphere above the disk plane, with density

$$n_H(z) = n_H(0) \exp \left[ \frac{-z^2}{2\sigma_h^2} \right], \quad (3)$$

where  $\sigma_h \approx R(\sigma_z/v_A)$  is the vertical scaleheight and  $\sigma_z = (18.1 \text{ km s}^{-1})T_{4.3}^{1/2}$  is the thermal velocity of hydrogen at temperature  $T = (10^{4.3} \text{ K})T_{4.3}$ . At a radius  $R = (100 \text{ kpc})R_{100}$  from the galactic center, we may express the total hydrogen density at the disk midplane as,

$$n_H(0) = \frac{N_H v_A}{(2\pi)^{1/2} \sigma_z R} = (3.57 \times 10^{-6} \text{ cm}^{-3}) N_{18} v_{50} R_{100}^{-1} T_{4.3}^{-1/2}, \quad (4)$$

where  $N_H = (10^{18} \text{ cm}^{-2})N_{18}$  is the total column density of hydrogen, neutral and ionized, integrated through the disk.

In the optically-thin limit, the neutral hydrogen density is set by photoionization equilibrium,

$$n(\text{H}^0) = \frac{n_e n_{H^+} \alpha_H^{(1)}}{\Gamma_H}, \quad (5)$$

where we adopt a case-A radiative recombination rate coefficient

$$\alpha_H^{(1)} = (2.48 \times 10^{-13} \text{ cm}^3 \text{ s}^{-1}) T_{4.3}^{-0.726} \quad (6)$$

and a hydrogen photoionization rate  $\Gamma_H = (2.64 \times 10^{-14} \text{ s}^{-1})I_{-23}$ . Here, we express the metagalactic ionizing radiation field,  $I_\nu = I_0(\nu/\nu_0)^{-\alpha_s}$ , with

$$I_0 = (10^{-23} \text{ ergs cm}^{-2} \text{ s}^{-1} \text{ Hz}^{-1} \text{ sr}^{-1}) I_{-23} \quad (7)$$

at  $h\nu_0 = 13.6 \text{ eV}$  and adopt a spectral index  $\alpha_s \approx 1.5$ . For a fully ionized gas with  $n_{He}/n_H = 0.1$  and  $n_e/n_H = 1.2$ , we find  $n(\text{H}^0) = (11.25)n_H^2 T_{4.3}^{-0.726} I_{-23}^{-1}$  and

$$N_{HI}(R) = (2.84 \times 10^{13} \text{ cm}^{-2}) N_{18}^2 v_{50} R_{100}^{-1} T_{4.3}^{-1.23} I_{-23}^{-1}. \quad (8)$$

Note that  $N_{HI}$  is proportional to  $N_H^2/R$ , owing to the  $n_H^2$  dependence of the recombinations that form H I. In the inner portions of disks, where the gas layer is optically thick to external ionizing radiation, the H I radial distribution,  $N_{HI}(R)$ , closely tracks that of total hydrogen,  $N_H(R)$ . However, in the extended disk, beyond the radius at which the integrated column of H I drops below several times  $10^{19} \text{ cm}^{-2}$ , the disk becomes optically thin to ionizing radiation, and the above photoionization analysis applies. In this regime, the radial H I distribution falls off as  $N_H^2/R$ , which in an exponential gaseous disk results in a very sharp falloff in H I. However, in disks with power-law gaseous distributions,  $N_H(R) \propto R^{-\Gamma}$  ( $1 \leq \Gamma \leq 2$ ), the H I decreases with radius as  $N_{HI}(R) \propto R^{-(2\Gamma+1)}$ .

Let us now compare these expectations to the observed Ly $\alpha$  absorbers, which typically have columns  $N(\text{H I}) \approx 10^{13-14} \text{ cm}^{-2}$ . From eq. (8), if the HST-observed Ly $\alpha$  cloud has H I column density  $10^{13.5} \text{ cm}^{-2}$  at  $R = (68 \text{ kpc})h^{-1}$ , the gaseous disk at that radius must have a total hydrogen column density

$$N_H(R) = (0.87 \times 10^{18} \text{ cm}^{-2})v_{50}^{-1/2}h^{-1/2}I_{-23}^{1/2}T_{4.3}^{0.61}, \quad (9)$$

assuming the optically-thin limit. The VLA observations of the dwarf H I galaxy toward Mrk 335 yield an H I column of  $N_0 = 2.4 \times 10^{19} \text{ cm}^{-2}$  at  $1'$ , corresponding to  $R_0 = 5.73h^{-1} \text{ kpc}$  at the recessional velocity of  $1970 \text{ km s}^{-1}$ . If we assume that the radial distribution of total hydrogen column density is  $N_H(R) = N_0(r/R_0)^{-1}$  (i.e.,  $\Gamma = 1$ ) and integrate over radii  $R_0 < r < R_{\text{max}}$ , where  $R_{\text{max}} = 68h^{-1} \text{ kpc}$ , the total gaseous mass of the extended disk is

$$M_{\text{disk}} = 2\pi N_0 \mu R_0 (R_{\text{max}} - R_0) = (6 \times 10^8 M_{\odot})h^{-2}, \quad (10)$$

where we adopt a mean molecular mass  $\mu = 1.4m_H$ .

The mass of the isothermal dark-matter halo required to confine the gas in equilibrium is given by,

$$M_{\text{halo}} = \frac{2\langle v^2 \rangle R}{G} = (4 \times 10^{10} M_{\odot})v_{50}^2 h^{-1}. \quad (11)$$

The ratio of halo mass to gas mass is therefore  $66v_{50}^2h$ , not dissimilar from values in other galaxies.

### 5.2. The PKS 2155-304 Sight Line

A possible physical association between the Ly $\alpha$  absorber at  $5100 \text{ km s}^{-1}$  seen toward PKS 2155-304 and ESO 466-G032 is even less clear cut. The projected distance between the two is  $230h^{-1}$  kpc. Lanzetta et al. (1995) find that only 1 out of 9 galaxies at projected distances larger than  $160h^{-1}$  kpc from the line of sight toward HST spectroscopic target QSO's gives rise to associated Ly $\alpha$  absorption, while 5 out of 5 galaxies at distances less than  $70h^{-1}$  kpc give rise to associated Ly $\alpha$  absorption. However more recent data by Bowen et al. (1996) and Le Brun et al. (1996) show that the covering factor of galaxies between 50 and  $300h^{-1}$  kpc is roughly 0.5 for equivalent widths larger than  $0.3 \text{ \AA}$ . Thus, our discovery does not seem that unusual.

The galaxy is a small Sb spiral with  $M = -19.2$ . It would be quite extraordinary if it had a gaseous halo extending out to 250 kpc or so. The long dynamic time scales at those distances make it unlikely that the gas has virialized or settled into a disk (Stocke et al. 1995). Note, however, that Zaritski & White (1994) find that isolated spirals have dark halos extending out to 200 or 300 kpc, thus even if the Ly $\alpha$  absorber is not part of a halo of ionized gas, it may still sit in the potential of the galaxy. As in the case of Mrk 335, the kinematics of the galaxy do not help to elucidate the situation, the Ly $\alpha$  absorber is at the systemic velocity of the galaxy.

In the high-velocity range toward PKS 2155-304, we see three galaxies at rather large projected distances from the line of sight. The three galaxies have a mean velocity of  $17,021 \text{ km s}^{-1}$  and a line of sight velocity dispersion of  $138 \text{ km s}^{-1}$ , typical of a loose group of

galaxies. The Ly $\alpha$  absorption at 17,100 km s $^{-1}$  occurs close to the mean velocity. In this case, it seems more plausible that the absorption arises in some general intergalactic gas within a small group, rather than from one galaxy in particular (Mulchaey et al. 1993, 1996). The galaxy to the southwest is in projection closest to the line of sight toward the quasar at a distance of  $305h^{-1}$  kpc. Thus, if the absorption arises in the halo of the nearest galaxy, the halo would have to extend well beyond 300 kpc. The existence of such a huge ionized halo is problematic by itself (Stocke et al. 1995), in a group environment it will definitely not survive. Of course the intragroup gas may be just that, the remains of the shredded halos. It is interesting that the absorption at 17,100 km s $^{-1}$  is one of the stronger absorption systems. The situation is reminiscent of the absorbers found toward 3C 273 in the outskirts of the Virgo cluster (Bahcall et al. 1991; Morris et al. 1991). Several galaxies are found at distances of 200 to 300 kpc from the sight line, but it is not possible to associate the absorbers with individual galaxies (Morris et al. 1993; Salpeter and Hoffman 1995; Rauch et al. 1996). As in the present case, the absorbers toward 3C 273 have slightly higher column density. Although the current data for the PKS 2155-304 system, plagued as they are by interference, are not sensitive enough to detect small gas rich dwarfs, such as the one found toward Mrk 335, the 3C 273 data definitely rule out the existence of such dwarfs within 100 kpc from the line of sight toward 3C 273 (van Gorkom et al. 1993).

The absorption at 16,488 km s $^{-1}$  seems more difficult to explain. It is quite far off from the mean velocity of the group. The H I emission from F21569-330 at a projected distance of  $610h^{-1}$  kpc comes closest in velocity going down to 16,650 km s $^{-1}$ , but not only is the distance to the sight line huge, the approaching side of the galaxy is on the far side from the sight line to the quasar. Since for this group we have only sampled the upper end of the H I mass function it is not unlikely that other galaxies are present which have H I at the same velocity as the absorber. Thus it seems plausible that this absorber is associated with the group as well.

In a recent paper Lanzetta, Webb and Barcons (1996) report the identification of a group of galaxies at a redshift of 0.26, that produce a complex of corresponding Ly  $\alpha$  absorption lines. As in the present case one of the absorption systems has a slightly higher column density. Thus it seems that Ly  $\alpha$  absorption arising in intra group gas may be quite common and that the column densities in those environments may be somewhat higher than what is seen near more isolated galaxies.

### 5.3. The Nature of Nearby Ly $\alpha$ Absorbers

A search for H I emission from the vicinity of nearby Ly $\alpha$  absorbers has resulted in the discovery of some low luminosity galaxies at the same redshift of some of the absorbers, but at large (70 to 250 kpc) projected distances from the sight line. In addition a group of galaxies was found near two absorbers at a velocity of about 17000 km s $^{-1}$ . This confirms previous suggestions that nearby Ly $\alpha$  absorbers are weakly correlated with galaxies. Individual, more isolated, galaxies may have absorbers that are physically associated with them, either due to infall, galactic winds or tidal disturbances. In regions of higher galactic density this material may be stripped from individual galaxies and distributed more uniformly through the intergalactic medium.

This project was undertaken in the hope of finding a possible parent population associated with nearby Ly $\alpha$  absorbers: either luminous galaxies with very extended gaseous envelopes or very low luminosity, but gas rich galaxies, which could have escaped optical detection. We did indeed find a few optically uncataloged galaxies, which turned out to be very close in velocity to, but at large projected distances from the Ly $\alpha$  absorbers. Two of the absorbers appear associated with a group of galaxies. These results are very similar to searches for a possible parent population at optical wavelengths. Most absorbers at low

redshift appear to coincide with the large scale structure outlined by the more luminous galaxies (Rauch et al. 1996; Stocke et al. 1995) as was first suggested by Oort (1981).

One of the outstanding questions is whether the nearby Ly $\alpha$  absorbers are actually connected to individual galaxies or simply coincide in redshift. Our observations do to a certain extent strengthen the idea that at least some nearby Ly $\alpha$  absorbers may be arising in mostly ionized halos of individual galaxies. The discovery in our most sensitive observation of a very small galaxy at  $68h^{-1}$  kpc from the line of sight toward Mrk 335, suggests that: (1) deeper surveys may turn up more such candidates; and (2) the suggestion (Maloney 1992; Shull et al. 1996) that the ionized halos of smaller galaxies may contribute significantly to the total Ly $\alpha$  absorbing cross section in the nearby universe may be valid. The strongest evidence for a physical connection between nearby Ly $\alpha$  absorbers and galaxies comes from the statistical work by Lanzetta et al. (1995), who showed that within  $70h^{-1}$  kpc from a galaxy there is a 100% chance of detecting Ly $\alpha$  absorption. There are however also some Ly $\alpha$  clouds with no optical galaxy within a few Mpc (Stocke et al. 1995; Shull et al. 1996). In one case, an anticorrelation between a region of high galaxy density and Ly $\alpha$  forest absorbing clouds has been found (Morris et al. 1991). The difference between these results may primarily be due to a difference in cloud column densities. The Lanzetta et al (1995) absorbers have significantly higher H I column densities than those studied by Morris et al. (1991), Stocke et al. (1995) and Shull et al. (1996).

Even if a physical connection is apparent, it is not obvious what the nature of the extended gas is. While Barcons et al. (1995) find in two cases Ly $\alpha$  absorption that could possibly be interpreted as arising in a corotating halo, there are several examples of even higher column density absorbers and metal lines, where the gas, although clearly associated with galaxies, is not corotating, but instead arises in tidally disturbed gas (e.g., Womble 1992; Carilli & van Gorkom 1992; Bowen et al. 1995). Thus the final verdict is not out yet.

Low column density gas is likely to be found near galaxies, and many possible scenarios can bring it there: retarded infall, outflow, corotating ionized disks, tidal disturbances. Quite likely, all of these occur. Perhaps most puzzling are the clouds that don't have any galaxies within many Mpc's. These may arise in the filamentary structures as produced in simulations of gravitational structure formation (Cen et al. 1994; Hernquist et al. 1996; Miralda-Escudé et al. 1996; Mücke et al. 1996), or they may be associated with as yet undetected dwarf galaxies.

This brings us to the final question, what is the connection, if any, between the high redshift Ly $\alpha$  forest clouds and nearby Ly $\alpha$  absorbers? As was pointed out by Rauch et al. (1996), the size estimate for coherent Ly $\alpha$  absorption at large redshifts (Bechtold et al. 1994; Dinshaw et al. 1994; Fang et al. 1996) is typically larger than the transverse separation between galaxies near low redshift Ly $\alpha$  absorbers. This not only argues against single extended galactic disks or halos as the main origin for the coherent absorption on large scales seen at high redshifts. It also argues against the low redshift absorbers being physically the same as the high redshift absorbers. However, it may well be that at low redshifts galaxies and absorption systems trace the general matter distribution on large scales, a hypothesis that can only be tested statistically using a large ensemble of nearby Ly $\alpha$  clouds.

JHvG thanks John Hibbard for comments on an earlier version of this manuscript and for stimulating discussions on the nature of Ly $\alpha$  clouds. We are grateful to Tony Foley for help with the WSRT observations. We thank the NFRA (Netherlands Foundation for Research in Astronomy) and the NRAO (National Radio Astronomy Observatory) for allocation of observing time. The NRAO is operated by Associated Universities, Inc. under a cooperative agreement with the National Science Foundation. This research was partly supported by NSF grant AST 90-23254 to Columbia University, a NOVA research

fellowship to CLC at the University of Leiden, and through a HST Guest Observer grant (GO-3584.01-91A) and the NASA Astrophysical Theory program (NAGW-766) at the University of Colorado. JHvG thanks the Astronomy Dept of Caltech, where part of this work was done, for hospitality, Wal Sargent and Nick Scoville for financial support, and Shri Kulkarni for entertainment. This research has made use of the NASA/IPAC extragalactic database (NED) which is operated by the JPL, Caltech, under contract with NASA.

## REFERENCES

- Allen, R. G., Smith, P. S., Anger, J. R., Miller, B. W., Anderson, S. F. & Margon, B. 1993, *ApJ*, 403, 610
- Bahcall, J. N., Jannuzi, B. T., Schneider, D. P., Hartig, G. F., Bohlin, R. & Junkkarinen, V. 1991, *ApJ*, 377, L5
- Bahcall, J. N. et al. 1993, *ApJS*, 87, 1
- Bajtlik, S. 1993, in *The Evolution and Environment of Galaxies*, ed. J. M. Shull & H. A. Thronson, (Dordrecht: Kluwer), 191
- Barcons, X., Lanzetta, K. M. & Webb J. K. 1995, *Nature*, 376, 321
- Bechtold, J. 1993, in *The Evolution and Environment of Galaxies*, ed. J. M. Shull & H. A. Thronson (Dordrecht: Kluwer), 559
- Bechtold, J., Crotts, A. P. S., Duncan, R. C. & Fang, Y. 1994, *ApJ*, 437, L83
- Bowen, D. V., Blades, J. C. & Pettini, M. 1995, *ApJ*, 448, 634
- Bowen, D. V., Blades, J. C. & Pettini, M. 1996, *ApJ*, 464, 141
- Briggs, F. 1990, *AJ*, 100, 999
- Bruhweiler, F. C., Boggess, A., Norman, D. J., Grady, C. A., Urry, C. M. & Kondo, Y. 1993, *ApJ*, 409, 199
- Carilli, C. L. & van Gorkom, J. H. 1992, *ApJ*, 399, 373
- Cen, R., Miralda-Escudé, J., Ostriker, J. P. & Rauch, M. 1994, *ApJ*, 437, L9
- Cornwell, T. J., Uson, J. M. & Haddad, N. 1992, *A&A*, 258, 583
- Dinshaw, N., Impey, C. D., Foltz, C. B., Weymann, R. J. & Chaffee, F. H. 1994, *ApJ*, 437,

- Dove, J. B. & Shull, J. M. 1994, *ApJ*, 423, 196
- Fang, Y., Duncan, R. C., Crotts, A. P. S. & Bechtold, J. 1996, *ApJ*, 462, 77
- Hernquist, L., Katz, N. Weinberg, D. H. & Miralda-Escudé J. 1996, *ApJ*, 457, L51
- Lanzetta, K., Bowen, D. V., Tytler, D. & Webb J. K. 1995, *ApJ*, 442, 538
- Lanzetta, K., Webb, J. K. & Barcons, X. 1996, *ApJ*, 456, L17
- Le Brun, V., Bergeron, J. & Boissé P. 1996, *A&A*, 306, 691
- Lu, L., Wolfe, A. & Turnshek, D. A. 1991, *ApJ*, 367, 19
- Lynds, R. 1971, *ApJ*, 164, L73
- Maloney, P. 1992, *ApJ*, 398, L89
- Maraschi, L., Blades, J. C., Calanchi, C., Tanzi, E. G. & Treves, A. 1988, *ApJ*, 333, 660
- Marzke, R. O., Huchra, J. P. & Geller, M. J. 1994, *ApJ*, 428, 43
- Miralda-Escudé, J., Cen, R., Ostriker, J. P. & Rauch, M. 1995, preprint
- Mo, H. J. & Morris, S. L. 1994, *MNRAS*, 269, 52
- Morris, S. L. & van den Bergh, S. 1994, *ApJ*, 427, 696
- Morris, S. L., Weymann, R. J., Dressler, A., McCarthy, P. J., Smith, B. A., R. J., Giovanelli, R. & Irwin, M. 1993, *ApJ*, 419, 524
- Morris, S. L., Weymann, R. J., Savage, B. D. & Gilliland, R. L. 1991, *ApJ*, 377, L21
- Mücket, J. P., Petitjean, P. & Kates, R. E. 1996, *A&A*, 308, 17
- Mulchaey, J. S., Davis, D. S., Mushotzky, R. F. & Burstein, D. 1993, *ApJ*, 404, L9
- Mulchaey, J. S., Mushotzky, R. F., Burstein, D. & Davis, D. S. 1996, *ApJ*, in press
- Oort, J. H. 1981, *A&A*, 94, 359
- Rao, S. & Briggs, F. 1993, *ApJ*, 419, 515

- Rauch, M., Carswell, R. F., Chaffee, F. H., Foltz, C. B., Webb, J. K., Weymann, R. J., Bechtold, J. & Green, R. F. 1992, *ApJ*, 390, 387
- Rauch, M., Carswell, R. F., Webb, J. K. & Weymann, R. J. 1993, *ApJ*, 260, 589
- Rauch, M., Weymann, R. J. & Morris, S. L. 1996, *ApJ*, 458, 518
- Salpeter, E. E. & Hoffman, G. L. 1995, *ApJ*, 441, 51
- Salzer J. J., 1992, *AJ*, 103, 385
- Sargent, W. L. W., Young, P. J., Boksenberg, A. & Tytler, D. 1980, *ApJS*, 42, 41
- Shull, J.M., Stocke, J. & Penton, S. 1996, *AJ*, 111, 72
- Smette, A., Surdej, J., Shaver, P. A., Foltz, C. B., Chaffee, F. H., Weymann, R. J., Williams, R. E. & Magian, P. 1992, *ApJ*, 389, 39
- Stocke, J. T., Shull, J. M., Penton, S., Donahue, M. & Carilli, C. 1995, *ApJ*, 451, 24
- Szomoru, A., Guhathakurta, P., Gorkom, J. H., Knapen, J. H., Weinberg, D. H. & Fruchter, A. S. 1994, *AJ*, 108, 491
- Szomoru, A. 1994, Ph.D. Thesis, University of Groningen
- Szomoru, A. van Gorkom, J. H., Gregg, M.D. & Strauss, M. A. 1996, *AJ*, 111, 2150
- Tytler, D., 1987, *ApJ*, 321, 49
- van Gorkom, J. H., Bahcall, J. N., Jannuzzi, B. T. & Schneider, D. P. 1993, *AJ*, 106, 2213
- Weinberg, D. H., Szomoru, A., Guhathakurta, P. & van Gorkom, J. H. 1991, *ApJ*, 372, L13
- Weymann, R. J. 1993, in *The Evolution and Environment of Galaxies*, ed. J. M. Shull & H. A. Thronson, (Dordrecht: Kluwer), 213
- Womble, D. S., 1992, Ph.D. Thesis University of California, San Diego

Zaritski, D. & White, S. D. M. 1994, ApJ 435, 599

Fig. 1.— Contour images of the velocity channels for the sight line toward Mrk 335. Only the area around the uncataloged dwarf, which was detected in H I emission is shown. The optical position of the galaxy center is shown with a cross, heliocentric velocities in  $\text{km s}^{-1}$  are indicated in the top right corner of each panel. The ellipse in the top left panel is the size of synthesized beam. Contour levels are -2, -1, 1, 2, 3, 4, 5, 6, 7 mJy per beam. Negative contours are dashed.

Fig. 2.— A position velocity plot along the major axis, taken at a position angle of  $0^\circ$ , of the dwarf in the Mrk 335 field. Contour levels are at -1.2, 1.2, 2.4, 3.6, 4.8, 6.0 mJy per beam.

Fig. 3.— An overlay of the H I emission (contours) on an image of the digitized POSS showing Mrk 335, lower left corner and the dwarf detected in H I. The contour interval is  $4.8 \times 10^{19} \text{ cm}^{-2}$ . The arrow points to Mrk 335.

Fig. 4.— Contour images of the velocity channels of ESO 466-G032, which is located close to the sight line of PKS 2155-304 at the same velocity as the absorber at  $5100 \text{ km s}^{-1}$ . The optical position of the galaxy center is shown with a cross, heliocentric velocities in  $\text{km s}^{-1}$  are indicated in the top right corner of each panel. The ellipse in the top left panel is the size of synthesized beam. Contour levels are -1.3, 1.3, 2.6, 3.9, 5.2 mJy per beam, negative contours are dashed.

Fig. 5.— An overlay of the HI column density distribution (contours) of ESO 466-G032 on an optical image (greyscale), which shows both the galaxy and PKS 2155-304. The contour interval is  $4.2 \times 10^{19} \text{ cm}^{-2}$ . The arrow points to PKS 2155-304.

Fig. 6.— Contour images of the velocity channels of the galaxy 2155-3033, south of PKS 2155-304. The optical position of the galaxy center is shown with a cross, heliocentric velocities in  $\text{km s}^{-1}$  are indicated in the top right corner of each panel. The ellipse indicates the size of the synthesized beam. Contour levels are -1.2, -0.6, 0.6, 1.2, 1.8 mJy per beam. Negative contours are dashed.

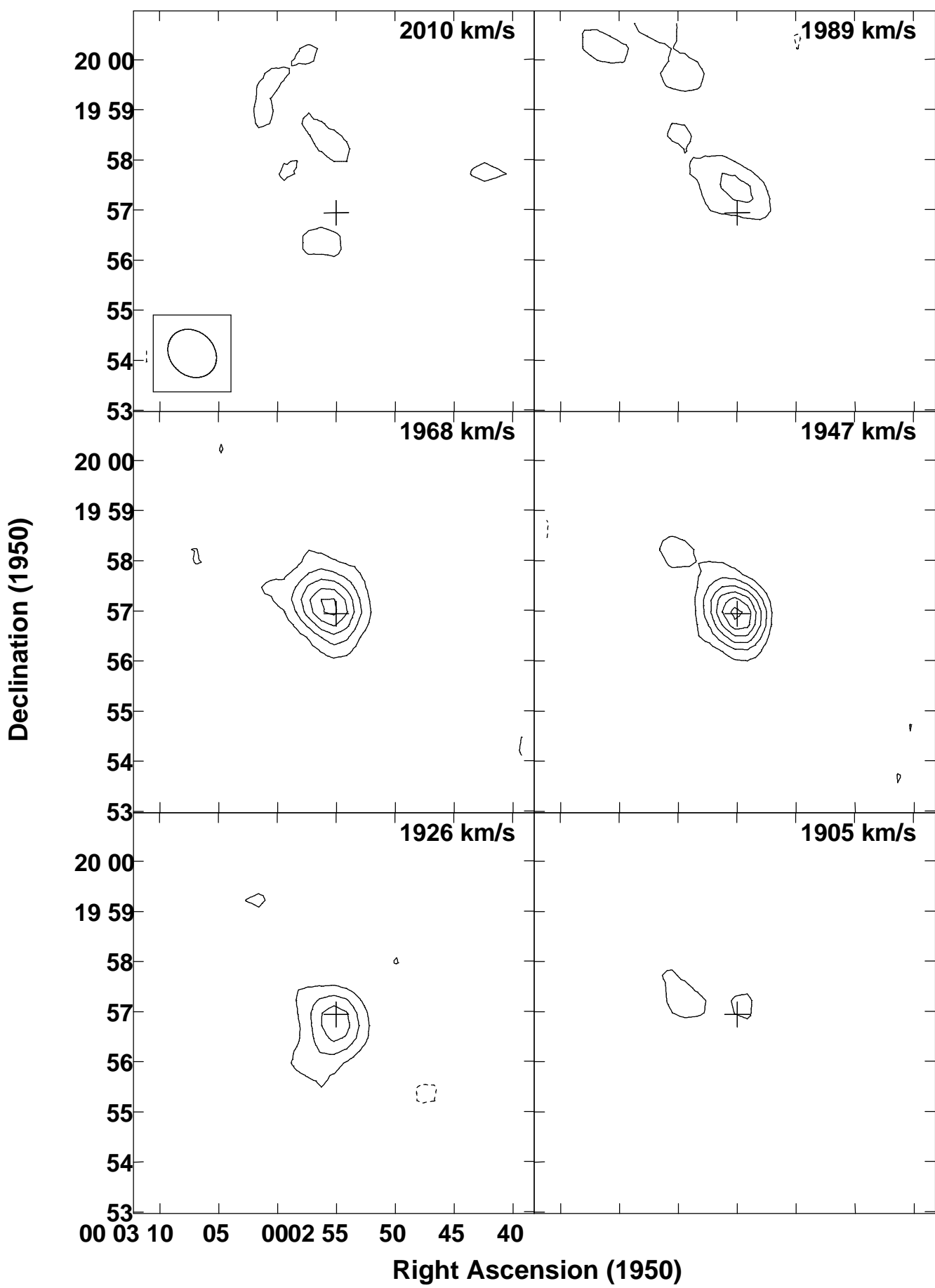
Fig. 7.— Contour images of the velocity channels of F21569-330, a galaxy to the south east of PKS 2155-304. The optical position of the galaxy is shown with a cross, heliocentric velocities in  $\text{km s}^{-1}$  are indicated in the top right corner of each panel. The ellipse indicates the size of the synthesized beam. The contour levels are -0.7, 0.7, 1.4, 2.1 mJy per beam. Negative contours are dashed.

Fig. 8.— A position velocity profile along the major axis of F21569-330 at a position angle of  $-40^\circ$ . Contour levels are -1,1,2,3 mJy per beam. Negative contours are dashed.

Fig. 9.— Contour images of the velocity channels of the galaxy north of PKS 2155-304. The cross indicates the optical position of the galaxy, heliocentric velocities ( $\text{km s}^{-1}$ ) are indicated in the top right corner of each panel. Contour levels are -0.7, 0.7, 1.4 mJy per beam. negative contours are dashed.

Fig. 10.— A position velocity profile along the major axis (east west) of the galaxy north of PKS 2155-304. Contour levels are -0.7, 0.7, 1.4 mJy per beam. Negative contours are dashed.

Fig. 11.— An overlay of the H I surface density distribution (contours) of the three galaxies detected in H I at velocities of about  $17000 \text{ km s}^{-1}$  on an optical image (greyscale), which shows the three galaxies and PKS 2155-304. The contour interval is  $2.34 \times 10^{19} \text{ cm}^{-2}$ . The arrow points to PKS 2155-304.



**TABLE 1.** Absorption Line Systems and “Associated” H I in Emission

Source	Velocity <sup>a</sup> km sec <sup>-1</sup>	Equivalent Width mÅ	Impact Parameter h <sup>-1</sup> kpc	Δ V <sup>b</sup> km sec <sup>-1</sup>
MKN 501	4660	154		
MKN 501	7530	48		
PKS 2155-304	5100	480	230	0
PKS 2155-304	16488	350		
PKS 2155-304	17100	810	305	0
Mrk 335	1970	170	68	20
Mrk 335	2290	73		

<sup>a</sup>Heliocentric corrected central velocity, optical definition.

<sup>b</sup>  $V_{Ly\alpha} - V_{sys}$  of nearest galaxy.

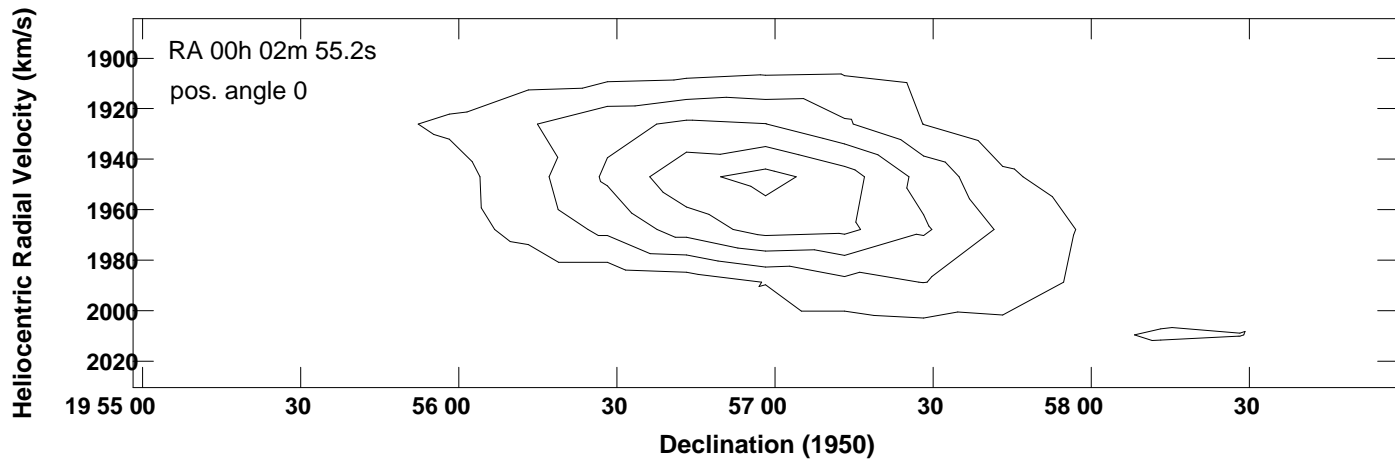


TABLE 2. Observing Log

Source	Telescope	Date	Configuration <sup>a</sup>	Velocity <sup>b</sup> km sec <sup>-1</sup>	Channel Width kHz	No. Channels	Integration Time Hours
MKN 501	WSRT	Dec. 18, 1993	54m	4675	78	63	12
MKN 501	WSRT	Jan. 9, 1994	36m	7530	78	63	12
MKN 501	WSRT	Feb. 3, 1994	36m	4675	78	63	12
PKS 2155-304	VLA	Sept. 26, 1993	DnC	5100	48.8	63	4
PKS 2155-304	VLA	Sept. 26, 1993	DnC	17400	48.8	63	3
PKS 2155-304	VLA	Sept. 30, 1993	DnC	17400	48.8	63	7
PKS 2155-304	VLA	Apr. 24, 1995	D	16880	195	31	6
PKS 2155-304	VLA	May 1, 1995	D	16880	195	31	6
Mrk 335	VLA	Apr. 24, 1995	D	2135	97.7	63	2
Mrk 335	VLA	May 1, 1995	D	2135	97.7	63	2

<sup>a</sup>Shortest WSRT spacing in meters, or VLA configuration.

<sup>b</sup>Heliocentric corrected central velocity, optical definition.

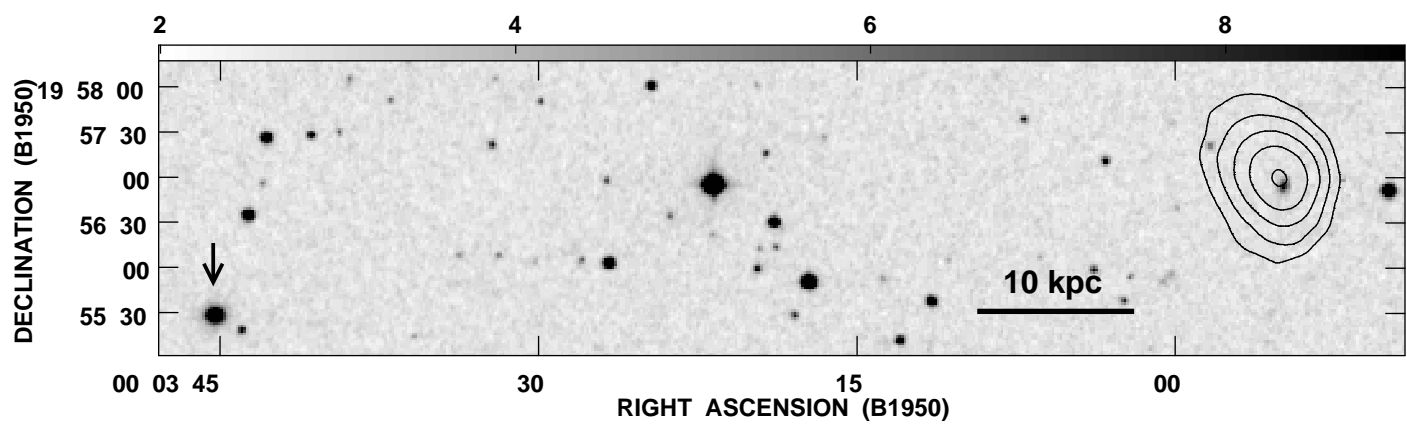


TABLE 3. Sensitivities

Source	Velocity Range km sec <sup>-1</sup>	Beam FWHM arcsec	Velocity Resolution km sec <sup>-1</sup>	Noise <sup>a</sup> mJy per beam	Mass <sup>b</sup> x10 <sup>7</sup> h <sup>-2</sup> M <sub>⊙</sub>	Column Density <sup>c</sup> x10 <sup>20</sup> cm <sup>-2</sup>
Mrk 501	4175 - 5175	25x15	34	0.55	5	2.7
Mrk 501	4175 - 5175	25x15	68	0.35	7	3.5
Mrk 501	4175 - 5175	38x38	34	0.90	8	1.1
Mrk 501	7030 - 8030	25x15	34	0.80	18	3.9
Mrk 501	7030 - 8030	25x15	68	0.55	25	5.5
Mrk 501	7030 - 8030	38x38	34	1.40	31	1.6
PKS 2155-304	4844 - 5409	66x39	21	0.60	4	0.3
PKS 2155-304	4844 - 5409	66x39	43	0.43	6	0.4
PKS 2155-304	17100 - 17723	53x45	46	0.23	34	0.2
PKS 2155-304	16283 - 17525	98x47	46	0.3	50	0.16
Mrk 335	1660 - 2660	63x53	25	0.40	0.5	0.16

<sup>a</sup>RMS per channel.

<sup>b</sup>5 $\sigma$  HI mass per beam per channel at the field center.

<sup>c</sup>5 $\sigma$  HI column density per channel at the field center.

## ESO 466-G032

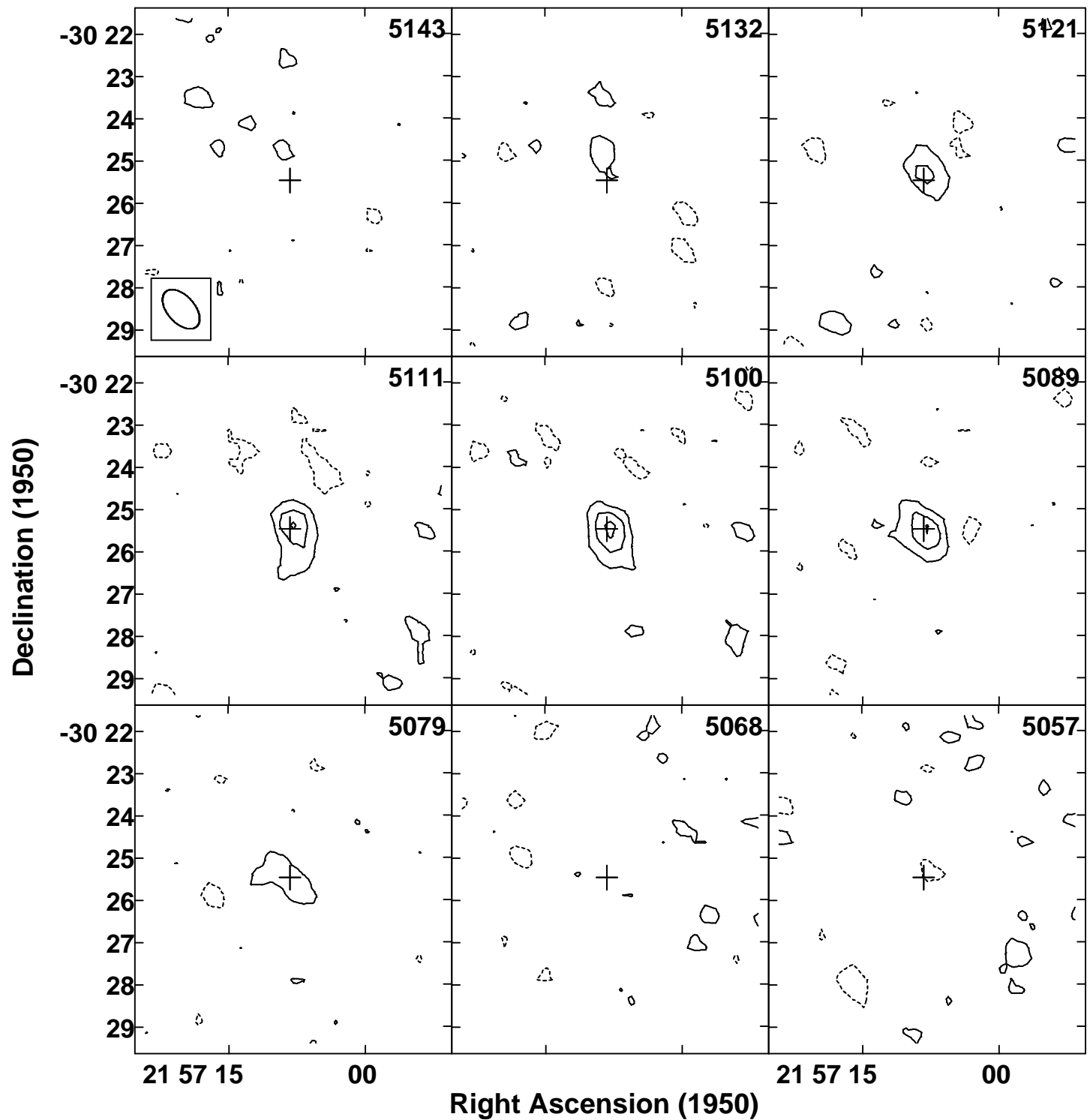
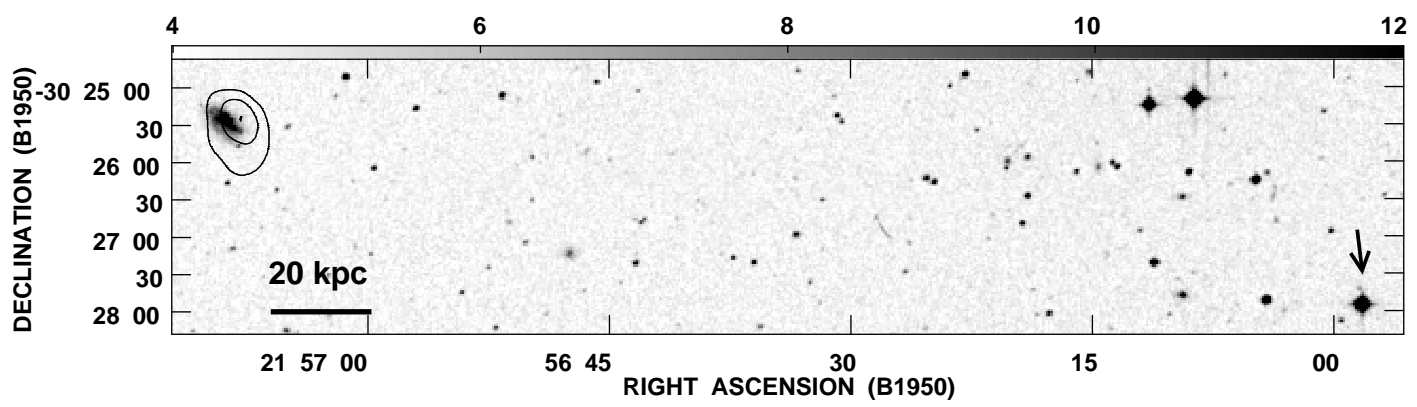
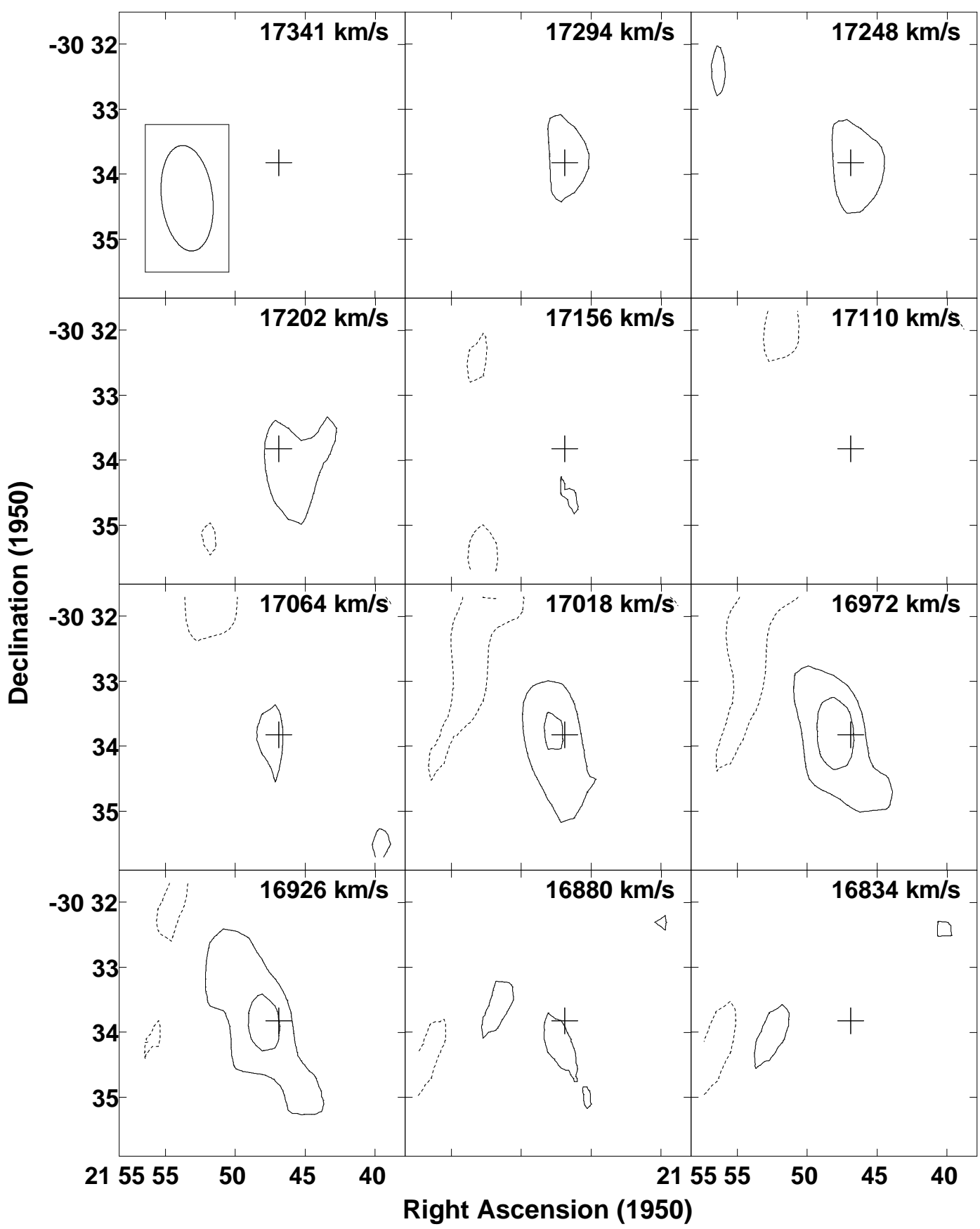


TABLE 4. Galaxies detected in H I

Sight line	Name	RA (1950) h m s	Dec (1950) ° ' ''	$V_{hel}$ km sec $^{-1}$	Velocity Range km sec $^{-1}$	$M_{H\,I}$ x10 $^8$ h $^{-2}$ M $_{\odot}$
Mrk 335	uncataloged	00 02 54.9	+19 56 54.3	1950	1926 - 1988	0.4
PKS 2155-304	ESO 466-G032	21 57 08.8	-30 25 25.8	5100	5076 - 5121	2.0
PKS 2155-304	2155-3033	21 55 46.9	-30 33 49.6	17100	16925 - 17293	28
PKS 2155-304	F21569-3030	21 56 56.0	-30 30 43.7	16788	16650 - 16925	80
PKS 2155-304	uncataloged	21 56 03.6	-30 17 08.7	17175	17063 - 17247	23



# 2155-3033



## F21569-330

